Published in final edited form as:

Oncogene. 2014 May 15; 33(20): 2620–2628. doi:10.1038/onc.2013.215.

Loss of N-Myc interactor promotes epithelial-mesenchymal-transition by activation of TGF-β/SMAD signaling

Daniel J. Devine[1], **Jack W. Rostas**[1,2], **Brandon J. Metge**[6], **Shamik Das**[6], **Madhuri S. Mulekar**[3], **J. Allan Tucker**[4], **William E. Grizzle**[6], **Donald J. Buchsbaum**[5], **Lalita A. Shevde**[6], and **Rajeev S. Samant**[6,†]

[1] Mitchell Cancer Institute, University of South Alabama, Mobile, Alabama

[2] Department of Surgery, University of South Alabama, Mobile, Alabama

[3] Department of Mathematics and Statistics, University of South Alabama, Mobile, Alabama

[4] Department of Pathology, University of South Alabama, Mobile, Alabama

[5] Department of Radiation Oncology, University of Alabama at Birmingham, Alabama

[6] Department of Pathology and Comprehensive Cancer Center, University of Alabama at Birmingham, Alabama

Abstract

Epithelial-Mesenchymal-Transition (EMT) is one of the critical cellular programs that facilitate the progression of breast cancer to an invasive disease. We have observed that the expression of N-myc interactor (NMI) decreases significantly during progression of breast cancer, specifically in invasive and metastatic stages. Recapitulation of this loss in breast cell lines with epithelial morphology [MCF10A (non-tumorigenic) and T47D (tumorigenic)] by silencing NMI expression causes mesenchymal-like morphological changes in 3-D growth, accompanied by up-regulation of SLUG and ZEB2 and increased invasive properties. Conversely, we found that restoring NMI expression attenuated mesenchymal attributes of metastatic breast cancer cells accompanied by distinctly circumscribed 3-D growth with basement membrane deposition and decreased invasion. Further investigations into the downstream signaling modulated by NMI revealed that NMI expression negatively regulates SMAD signaling, which is a key regulator of cellular plasticity. We demonstrate that NMI blocks TGF-β/SMAD signaling *via* up-regulation of SMAD7, a negative feedback regulator of the pathway. We also provide evidence that NMI activates STAT signaling which negatively modulates TGF-β/SMAD signaling. Taken together, our findings suggest that loss of NMI during breast cancer progression could be one of the driving factors that enhance invasive ability of breast cancer by aberrant activation of TGF-β/SMAD signaling.

† Corresponding author: Department of Pathology, WTI-320E, 1720, Second Avenue S. Birmingham, AL 35294 Phone: 205-975-6262 rsamant@uab.edu.

Daniel J. Devine: *Current Address:* St. Jude Children's Research Hospital, Department of Oncology, 262 Danny Thomas Blvd. Memphis, TN 38105

Keywords

N-Myc interactor; EMT; SMAD; Breast cancer

Introduction

One of the most lethal attributes of cancers such as breast cancer is its ability to spread to tissues far from its site of origin and colonize those tissues to form metastases (1). In recent years, epithelial-to-mesenchymal transition (EMT) has received a great deal of attention due to its ability to impart invasive potential to otherwise confined epithelial cells within a carcinoma (2, 3). The phenomenon of EMT was first observed when lens epithelial cells were suspended in a collagen matrix and the cells dramatically changed morphology and lost their distinctive epithelial polarity (4). Since that time, an enormous body of evidence has been generated that supports a physiological need for epithelial-to-mesenchymal transitions, particularly in embryonic development and wound healing (5). However, this otherwise elegant cellular program has also been implicated in pathologies, such as tissue fibrosis and cancer (6, 7). EMT is involved in the progression of several solid tumors such as prostate cancer, pancreatic cancer, colon cancer and breast cancer (8-14). Thus it is vitally important to find novel molecules involved in both positive and negative regulation of EMT.

TGF-β/SMAD signaling is one of the central pathways involved in regulating EMT. TGF-β ligands from the tumor microenvironment activate TGF-β receptors which in turn activate intracellular signal transducers, the SMAD family members, specifically R-SMAD 2 and 3. These together with SMAD 4 (co-SMAD) translocate to the nucleus and initiate a transcription program thought to be responsible for mesenchymal transition. The inhibitory SMADS (I-SMADs) *viz*. SMADs 6 and 7 provide negative feedback to prevent aberrant activation of this pathway (15). Abnormal activation of TGF-β signaling has been reported in late stage cancers including breast cancers (16, 17). This activation has been one of the key events in rendering breast cells invasive and presumably facilitating the initiation of EMT (18).

In this study, we propose a novel regulator of the epithelial state in breast cancer, the N-Myc interactor (NMI). NMI was first identified as a molecule capable of interacting with N-Myc (19). NMI is known to be capable of influencing important cellular signaling events such as modulation of STAT signaling (20) and negative regulation of hTERT transcription *via* its interaction with BRCA1 (21). We had previously observed that ectopic expression of NMI in highly tumorigenic and metastatic cell lines led to reduced *in vivo* tumor growth (in xenografts) and caused inhibition of Wnt/β-catenin signaling by enhancing degradation of non-membranous β-catenin (22). Here we present our observations that NMI expression is compromised in advanced breast cancer. We describe that modulation of NMI levels alters epithelial attributes; specifically loss of NMI expression promotes EMT. Conversely, restoration of NMI expression inhibits the mesenchymal phenotype. We present evidence that these effects of NMI are mediated by its inhibitory activity on TGF-β/SMAD signaling.

Results

NMI expression in breast cancer patients

NMI levels in breast cancer specimens have never been evaluated. We assessed NMI expression at the transcript level by quantitative RT-PCR analysis **(Figure 1A)** as well as at the protein level by immunohistochemically staining tissue-microarrays **(Figure 1B)**. Our analysis revealed a noticeable reduction in NMI expression in invasive breast cancer. NMI transcript levels were significantly lower in grade 2 and grade 3 breast cancer specimens compared to the levels in normal breast tissue. Similarly the immunohistochemical staining intensity and overall NMI staining showed a significant reduction in metastatic specimens as compared to the normal or fibroblastic breast tissue. We then analyzed the NMI protein level from 10 different breast cancer cell lines compared to human mammary epithelial lines (HME, HMEC and MCF10A). As observed in **Figure 1C**, some of these cell lines (MCF10CA.cl.d, MDA-MB-231, 2LMP) showed a noticeable reduction, others (MDA-MB-134, MDA-MB-453, MCF10CA.1a.cl.1) showed a total loss of NMI expression. However there were some cell lines (MCF7, T47D, BT20, MDA-MB-468) which retained NMI expression. A closer look at the reported status of the morphologic status and invasive attributes of these cell lines [based on reports by Neve *et al* and Blick *et al* (23, 24)] revealed that cell lines that display predominantly epithelial characteristics retain expression of NMI; however cell lines that are mesenchymal-like, display a noticeable loss of NMI protein expression **(Table 1)**.

Silencing NMI expression increases invasive ability

To gain insight into the implications of loss of NMI expression, we stably silenced NMI expression from the human breast epithelial cell line, MCF10A (non-tumorigenic). Conversely, we stably restored NMI expression in its isogenic, tumorigenic, and metastatic variant MCF10CA1.d (which expressed low endogenous levels of NMI). The resultant cell lines were termed as MCF10A-shNMI and MCF10CA1.d-NMI respectively and were tested for their invasive ability using a modified Boyden chamber assay. Our findings revealed that NMI-silenced cells showed approximately 2.2-fold increase in their invasive ability compared to the corresponding non-targeting control. In contrast, the NMI overexpressing cells displayed reduced invasive ability (45% of control) **(Figure 2 A & B)**.

Silencing NMI expression induces mesenchymal attributes

Three-dimensional cell culture models provide an environment in which epithelial cells form spherical structures, exhibit apical-basal polarity, and secrete a basement membrane that surrounds each structure (25). Non-invasive cells display predominantly spherical structures that are well contained within their basement membranes. In contrast, invasive cells will detach from surrounding cells, degrade the basement membrane, and invade into the surrounding matrix. When tested for growth in 3-D culture, the MCF10A non-targeting control transfected cells predominantly showed well preserved acinar structures whereas MCF10A-shNMI formed invasive structures **(Figure 2C)**. Staining of these 3-D structures for laminin-V to assess the integrity of the basement membrane revealed that while the non-targeting control cells had mostly intact basement membrane, MCF10A-shNMI had clearly discontinuous laminin-V staining indicative of a disrupted basement membrane **(Figure**

2C). On the contrary, NMI expression in MCF10CA1.d elicited a dramatic change in both, the size and shape of the resultant 3-D structures. The MCF10CA1.d-NMI cells produced much smaller and highly circumscribed (well preserved ascinar structures) 3-D structures, while the vector control cells produced large, irregularly-shaped, branching structures **(Figure 2D)**. There was minimal laminin-V staining of the control 3-D structures, indicative of disrupted basement membrane, while the NMI-expressing cells showed noticeable restoration of basement membrane **(Figure 2D)**.

Examination of some of the key molecular attributes of EMT revealed that silencing NMI expression resulted in increased expression of EMT-inducing transcription factors. NMI-silenced MCF10A cells showed an increased expression of mesenchymal transcription factors SLUG and ZEB2 simultaneous with downregulation of E-cadherin and keratin-18 **(Figure 2E)**. Conversely, expression of NMI in MCF10CA1.d decreased expression of EMT-inducing transcription factors SLUG and ZEB2 concomitant with increased expression of the epithelial marker keratin-18 **(Figure 2F)**.

In corroboration with the NMI silencing effect observed in MCF10A, T47D-shNMI cells (generated by silencing NMI expression from tumorigenic, non-metastatic T47D breast cancer cells) showed increased invasive ability **(Supplementary Figure 1 A)**. These cells also displayed altered cell morphology in 2-D growth (tissue culture plates). NMI silenced MCF10A and T47D cells, showed more lanceolate (spindle-like) appearance resembling mesenchymal like phenotype **(Supplementary Figure 1 B)**. These spindle like T47D-shNMI cells were noticeably devoid of E-cadherin staining **(Supplementary Figure 1C)**. While there was no concomitant gain of N-cadherin or vimentin, we did notice a gain of expression of mesenchymal transcription factors (SLUG and SNAIL) **(Supplementary Figure 1D)**.

NMI negatively regulates TGF-β/SMAD Signaling

The synergy between active TGF-β signaling and EMT is well documented (26); more specifically SLUG and ZEB2 expression are increased by active TGF-β/SMAD signaling (27, 28). Thus, we pursued the possibility that NMI influences EMT by regulating TGF-β signaling. Evaluation of SMAD-mediated transcriptional activity using SBE-4 reporter assays revealed that silencing NMI expression enhanced SMAD-mediated transcription approximately 5-fold in MCF10A and 3-fold in T47D. Conversely, NMI overexpression had a noticeable inhibitory effect on SMAD mediated transcription as seen by suppressed SBE-4 activity in MCF10CA1.d NMI cells **(Figure 3A)**.

To confirm the effect of NMI expression on TGF-β signaling, we analyzed levels of transcripts of known TGF-β/SMAD driven transcription target genes (PLAU, PTHLH, TGFBI and TGFBR3). We observed that expression of these genes increased in NMI-silenced cells and decreased in NMI expressors **(Figure 3B)**, confirming that signaling through the TGF-β/SMAD was upregulated upon loss of NMI expression.

Abrogating NMI expression increased the invasive ability MCF10A and T47D cells to an extent that was comparable to the respective shSCR cells treated with TGF-β1 ligand. (Note: sh-NMI invasion value in control group is comparable to the shScr values in TGF-β1 treated

group) **(Figure 3C & D)**. To determine if the increased invasive ability of NMI-silenced cells was an effect of increased TGF-β/SMAD signaling, we assessed the effect of TGF-β inhibitors (A8301 and SB) on the invasive ability of these cells. Treatment with either A8301 or SB resulted in significant loss (over 50%) of the invasive ability of the NMI-silenced cells **(Figure 3C & D)**. Consistent with the loss of invasive ability, a corresponding loss of ability to show invasive 3-D growth was noted in MCF10A-shNMI cells treated with A8301 **(Figure 3E)**. Western blot analysis of A8301 treated shNMI cells revealed decrease in SLUG and concomitant increase in keratin 18 expression **(Figure 3 E)**.

NMI regulates TGF-β/SMAD signaling via STAT5 mediated upregulation of SMAD7

NMI expression is up-regulated by IFN-γ (22). Also, NMI has been shown to augment STAT5 signaling downstream of IFN-γ (20). Hence, we assessed response of two different STAT5 regulated promoters, LHRE (lactogenic hormone response element) and β-casein, to STAT5 inhibitor treatment of MCF10CA1.d-NMI cells. We found that NMI expression led to a 2-fold increase in promoter activity of LHRE **(Figure 4A)** and 3-fold increase in promoter activity of β-casein **(Figure 4B)**, which was significantly ablated by STAT5 inhibitor treatment **(Figure 4 A & B)**. Upon STAT5 inhibition MCF10CA1.d-NMI cells regained the ability to invade **(Figure 4 C)** and showed increased expression of SLUG and ZEB2 **(Figure 4 D)**.

IFN-γ/STAT signaling antagonizes TGF-β/SMAD signaling (29, 30). This antagonistic effect has been attributed to IFN-γ mediated up-regulation of an inhibitory SMAD, SMAD7 (31). In NMI silenced cells SMAD7 protein levels were notably reduced whereas NMI overexpression increased SMAD7 protein expression **(Figure 4E)**. Hence, we used the approach of silencing SMAD7 expression in MCF10CA1.d-NMI cells to test its relevance to the signaling downstream of NMI. Upon SMAD7 silencing, these cells showed increased invasive ability **(Figure 4 F)** as well as increased expression of ZEB2 and the TGF-β target gene TGFBR3 **(Figure 4 G)**. These observations indicate that up-regulation of SMAD7 by NMI may mediate the negative impact of NMI on TGF-β/SMAD signaling.

Discussion

Cellular plasticity observed in the trans-differentiation process of EMT is integral to development, but it is also recapitulated in invasion and metastasis of carcinomas (32-34). EMT imparts invasive capacity to epithelial cells within a carcinoma, and thus it is thought to be a very important phenomenon underlying metastatic dissemination. A cell orchestrates this transition after integrating specific stimuli from several sources and converting those signals into distinct inter- and intra-cellular events. The best studied events are changes in gene expression that lead to functional phenotypic alterations. Several genes are repressed during EMT, including E-cadherin, the main molecular fastener of adherens junctions, and keratins (8 and 18), which are expressed by differentiated epithelial cells. Conversely, a host of genes are up regulated during EMT, several of which are transcription factors that mediate further downstream gene expression changes, while others are genes that directly aid the transition and provide the cell with the machinery necessary for becoming a

mesenchymal cell (35-37). Specifically of importance to this work, EMT plays a key role in breast cancer progression (9, 38).

Several signaling pathways such as Wnt, NFκβ, Hedgehog and Notch are significant drivers of EMT (39). More importantly, TGF-β signaling has been shown to play a central role in EMT. Several studies support a critical role of SMADs in TGF-β-dependent EMT associated tumor progression and metastasis (26, 40, 41). For example, antagonizing SMAD signaling decreased metastatic potential of xenografted breast cancer cell lines (42, 43); whereas overexpression of SMADs 2 and 3 resulted in increased EMT in a mammary epithelial model (44, 45). Multiple transcription factors that promote induction of mesenchymal phenotype, such as ZEB1, ZEB2, and SNAI1, are induced by TGF-β/SMAD signaling and play critical roles in TGF-β-induced EMT (40, 46). Thus overall, the TGF-β/SMAD signaling axis plays a key role in regulating critical EMT genes and breast cancer progression (47).

Despite its reported interactions with several key players in tumor progression and metastasis such as BRCA1, STATs, c-Myc, N-Myc, TIP60 and SOX10, only limited knowledge has been established about the mechanistic and functional role of NMI in tumor progression. We have discovered that NMI modulates TGF-β/SMAD signaling. The enhanced invasive ability of NMI-silenced cells is completely abrogated by treatment with TGF-β inhibitors. The levels of inhibitory SMADs (I-SMADs) are critical to regulating SMAD signaling. SMAD7 is an I-SMAD, that is up-regulated by NMI, antagonizes TGF-β signaling through multiple mechanisms. Overexpression of SMAD7 prevents injury-induced EMT of lens epithelial cells (48) and mammary epithelial cells (45). SMAD7 binds the TGF-β type I receptor (TβRI), interferes with recruitment, downstream phosphorylation and activation of the receptor-SMADs (R-SMADs), SMAD2 and 3 (49). Additionally, SMAD7 functions to recruit E3 ubiquitin ligases to TβRI, resulting in its degradation (50). Recent studies have demonstrated that repression of SMAD7 by the miR106b-25 cluster activates TGF-β signaling and induces EMT (51).

Both, the TGF-β/SMAD and the prolactin/JAK/STAT pathway are critical to the proper development, maintenance, and functioning of the mammary epithelial tissue. Interestingly, opposing physiological effects between these two signaling pathways are prominent in the regulation of mammary gland development. Activated r-SMADs inhibit STAT5 association with its co-activator CREB-binding protein, thus blocking STAT5 transactivation of its target genes and leading to inhibition of mammary gland differentiation and lactation (52). In fact, STAT and SMAD signaling pathways crosstalk with each other with interweaved regulatory mechanisms (53).

NMI is an IFN-γ up-regulated protein (22); and hence it is noteworthy that IFN-γ has been reported to abrogate TGF-β signaling (30, 54). This antagonistic regulation of TGF-β/SMAD signaling by IFN/STAT signaling is due to up-regulation of SMAD7 (31). Consistent with these reports, our studies reveal that NMI expression up-regulates SMAD7 and this up-regulation happens *via* enhancement of STAT signaling by NMI. [In our system, expression of other inhibitory SMAD, SMAD6, did not change (data not shown)]. We have also shown that NMI has an inhibitory effect on Wnt/β-catenin signaling (22). In that study we had

evaluated the functional implications of up-regulation of NMI expression in MDA-MB-231 breast cancer cells and MDA-MB-435 cells. We had observed a significant reduction in primary tumor growth in xenograft studies. We analyzed MDA-MB-231-NMI (231-NMI) cells for SMAD signaling activity using SBE-4 luciferase reporter assays. Consistent with our observations the cells restored for NMI significantly (65%) decreased activity of SBE-4 **(Supplementary Figure 2A)**. We had previously reported that these 231-NMI cells lacked invasive ability (22). When analyzed for the 3D growth morphology 231-NMI cells showed a striking absence of invasive, stellate outgrowth in cells with gain of a basement membrane stained with laminin V **(Supplementary Figure 2B)**.

Histological analysis of slow growing 231-NMI xenograft tumors compared to 231-Vector control tumors showed a well circumscribed tumor with minimal inflammation of the stroma and minimal invasion of surrounding tissue **(Supplementary Figure 2C)**. These cells were also deficient in their ability to colonize the lungs **(Supplementary Figure 2D)**. This reduced experimental metastasis may be the result of negative effect on proliferation as a consequence of suppression of canonical Wnt signaling or it may be due to the reduced ability of 231-NMI cells to invade the lung tissue. Wnt/β-catenin signaling is also a critical player in promotion of the EMT program. Thus the EMT effect upon loss of NMI could partly be a consequence of aberrant Wnt signaling. Several recent reports indicate that Mesenchymal-Epithelial-Transition (reversal of EMT) is necessary for overt metastatic growth (35, 55, 56). However, the effect of re-expression of NMI after the tumor cells invade the metastatic niche needs further assessments.

Thus we conclude that NMI is not just a binding partner of several transcription factors, but instead its expression has important functional consequences that impact malignant progression. Certainly, absence of NMI primes breast cancer cells to undergo EMT and prompts their metastatic dissemination. Our studies presented here provide a new insight into the role of the NMI as one of the gatekeepers of epithelial plasticity. Not only is this the first report of NMI regulating EMT, but it also pioneers the connection between NMI and the TGF-β signaling pathway. This exciting new discovery provides us with an insight into the mechanistic underpinnings of NMI's ability to have such profound effects on cellular behavior, and consequently revealing how its absence may contribute to the invasion of breast tumors. This also suggests a possibility that absence of NMI may indicate poor prognosis.

Materials and Methods

Cell Culture and Stable Cell Line Selection

HMEC and HME cell lines were grown in DMEM/F-12 (Life Technologies, Grand Island, New York) supplemented with 10ng/ml EGF (Sigma, St. Lous, MO), 500ng/ml Hydrocortisone (Sigma, St. Louis, MO), and 10ug/ml Insulin (Sigma, St. Louis, MO). MCF10A, MCF10CA1acl.1, and MCF10CAcl.d cells were grown in DMEM/F-12 supplemented with 5% Horse Serum (Life Technologies, Grand Island, New York), 100ng/ml Cholera Toxin (Sigma, St. Louis, MO), 10ug/ml Insulin, 25ng/ml EGF, and 500ng/ml Hydrocortisone. T47D cells were grown in RPMI 1640 media (Life Technologies, Grand Island, New York) supplemented with 10% FBS (Atlanta Biologicals, Norcross, GA),

10ug/ml Insulin, and 1% L-glutamine (Life Technologies, Grand Island, New York) . MCF-7 cells were grown in DMEM/F-12 supplemented in 10% Horse Serum and 10ug/ml Insulin. BT-20 cells were grown in EMEM (Life Technologies, Grand Island, New York) supplemented with 10%FBS, 1%L-glutamine, 1% sodium-Pyruvate (Life Technologies, Grand Island, New York) , and 1% Non-essential amino acids (Life Technologies, Grand Island, New York). MDA-MB-468 and MDA-MB-453 were grown in DMEM/F-12 supplemented with 10% FBS. MDA-MB-134 cells were grown in DMEM/F-12 supplemented with 20% FBS. 2LMP cells were grown in Improved MEM (Life Technologies, Grand Island, New York) supplemented with 10% FBS and 1% L-glutamine. MDA-MB-231 and MDA-MB-435 were grown in DMEM/F-12 supplemented with 5%FBS. All cells were grown in a 37°C humidified incubator with 5% CO_2. Stable silencing of NMI expression was accomplished using short-hairpin RNA cloned into pSuper.retro.puro vector (OligoEngine, Seattle, WA). Vector containing a non-targeting shRNA was used as a control. NMI overexpression in MCF10CA1.d was accomplished by cloning NMI cDNA into pIRESpuro3 (Clontech, Mountain View, CA) and the empty vector was used as a control. Vectors were transfected using Lipofectamine 2000® reagent (Invitrogen, Carlsbad, CA). Cells were selected in media supplemented with 500 ng/mL of puromycin (EMD Chemicals).

qRT-PCR Patient Tissue Arrays

TissueScan™ Breast Cancer and Normal Tissue cDNA Arrays (Origene USA, Rockville, MD) were used to analyze the transcript levels of N-Myc interactor (NMI). NMI transcript was probed using TaqMan® Gene Expression Assays (Hs00190768_m1) and TaqMan® Universal PCR Master Mix (Life Technologies). NMI Ct values were normalized to β-actin by calculating a ratio of actin C_t/NMI C_t. Significance was evaluated using one-way ANOVA followed by Dunnett's Multiple Comparisons Test.

Immunohistochemistry

Tissue microarray sides were obtained from the National Cancer Institute CBTR. Slides were heated at 60° C for 1 hour, followed by paraffin removal with xylene and subsequent rehydration with Tris-buffered saline (TBS). Antigen retrieval was performed in a chamber containing citrate buffer (pH 6.0) for 20 minutes at 97° C (DAKO PTlink, Carpinteria, CA). Samples were blocked with 3% hydrogen peroxide and 10% goat serum for 10 minutes each at room temperature. Sections were incubated at room temperature in primary antibody (NMI monoclonal, Sigma-Aldrich, 1:1200) for 30 minutes, an HRP-linked secondary antibody (Envision, DAKO, Carpinteria, CA) for 15 minutes, and 3,3-diaminobenzidine for 5 minutes. Samples were counterstained with hematoxylin, dehydrated, and mounted with a cover slip was applied.

Staining was scored via the Allred system. All samples were digitally imaged and scored (Automated Cellular Imaging System “ACIS”, DAKO, Carpinteria, CA) with the assistance of our collaborating pathologist (JAT). A proportion score was assigned that represents the estimated proportion of positive tumor cells on the entire slide as determined by the ACIS: no staining = 0; 0 to less than 1% = 1; 1% to less than 10% = 2; 10% to less than 33.3% = 3; 33.3% to less than 66.6% = 4; over 66.6% = 5. An intensity score, as determined by the

ACIS, was obtained of the average staining intensity of positive tumor cells: negative = 0; weak = 1; intermediate = 2; and strong = 3. The proportion score and the intensity score were added to obtain a total score (range of 0 to 8).

Protein Isolation and Immunoblotting

Cell lysates were collected on ice using NP-40 alternative (EMD Chemicals) combined with protease and phosphatase inhibitors (EMD Chemicals). Cell lysates were incubated on ice for 2 hours and then centrifuged at 13,000 RPM for 30 minutes. Protein concentration was estimated using PrecisionRed® (Cytoskeleton Inc., Denver, CO). Lysates were resolved on SDS-PAGE gels and transferred to PVDF membrane (Bio-Rad Laboratories, Hercules, CA). The membranes were blocked in either 5% non-fat dry milk or bovine serum albumin (Sigma-Aldrich), and probed with appropriate antibodies. The signal was visualized using SuperSignal® West Dura (Thermo Scientific, Rockford, IL) and documented using G:Box Chemi imager using the GeneSnap software (Syngene USA, Frederick, MD).

Primary antibodies for KRT18 (#4546), SLUG (#9585), SNAIL (#3895), GAPDH (#2118L), SMAD6 (#9519), TGFBI (#5601), TGFBR3 (#5544), α/β-tubulin (#2148) (Cell Signaling Technology, Inc., Danvers, MA) were used (dilution of 1:1000) in TBST (0.1% Tween) with 5% bovine serum albumin (Sigma-Aldrich). NMI (WH0009111M1) and ZEB2 (AV33694) primary antibodies (Sigma-Aldrich) were used in TBST (0.05% Tween) with 5% non-fat dry milk. The SMAD7 (MAB2029) and PLAU (MAB1310) primary antibodies (R&D Systems, Minneapolis, MN) were used according to the manufacturer's recommendations. Anti-mouse (NA931V) and anti-rabbit (NA934V) secondary antibodies (GE Healthcare, Pittsburgh, PA) were used at a 1:2500-1:5000 dilution.

Invasion Assays

Cells suspended in serum-free media were seeded in Biocoat® Matrigel® invasion chambers (BD Biosciences, Sparks, MD) according to the manufacturer's recommendations. Fibronectin (10 μg/mL) (BD Biosciences) was used as the chemoattractant. Cells were incubated at 37°C with 5% CO_2 for 10-12 hours. After incubation, cells were fixed in 4% paraformaldehyde (Boston Bioproducts, Ashland, MA) for 10 minutes at room temperature or overnight at 4°C. Cells were then stained with crystal violet (BD Biosciences) for 10 minutes at room temperature, rinsed with water, and allowed to dry overnight before imaging. Images were obtained and invaded cells were counted using the NIS Elements® software. Eight fields were counted for each group and statistical analysis was performed using GraphPad Prism® software. Significance was analyzed using one-way ANOVA and p values were calculated using Bonferroni's Multiple Comparison Test.

3-D Cell Culture

Cells suspended in growth media were seeded into an eight-chambered borosilicate cover glass system (Nalge Nunc International, Rochester, NY) coated with 3-D Culture Matrix™ reduced growth factor basement membrane extract (Trevigen Inc., Gaithersburg, MD). Five thousand cells that were suspended in 400 μl of growth media supplemented with 2% 3-D Culture Matrix™ were seeded in each chamber. Cells were incubated at 37°C with 5% CO_2 and growth media was changed every 3-4 days. Images of the acinar structures were

obtained 7-12 days after seeding (timing is cell line dependent). Laminin-V was visualized using Alexa Fluor® 488-conjugated anti-laminin-V (clone D4B5) (Millipore, Billerica, MA) and nuclei were stained with Vectashield® Hard Set ™ Mounting Medium with DAPI (Vector Laboratories, Inc., Burlingame, CA).

RNA isolation and quantitative real-time PCR

Total RNA was harvested using the RNEasy kit (Qiagen Inc., Valencia, CA). RNA (2 μg) was transcribed into complementary DNA using the High Capacity cDNA Reverse Transcription kit (Applied Biosystems, Foster City, CA). Quantitative real-time PCR was performed with TaqMan® Universal PCR Master Mix (Applied Biosystems) in an iCycler iQ5 (Bio-Rad Laboratories) real-time PCR detection system. TaqMan® Gene Expression Assays (Life Technologies) were used for the following genes: GAPDH (Hs99999905_m1), KRT18 (Hs01941416_g1), NMI (Hs00190768_m1), PLAU (Hs01547054_m1), SNAIL (Hs00195591_m1), SLUG (Hs00950344_m1), TGFBI (Hs00932747_m1), TGFBR3 (Hs01114253_m1), ZEB2 (Hs00207691_m1). Data collected was normalized to the endorsed control gene, GAPDH, and expressed as fold change in relative expression using the $\Delta\Delta C_t$ method ($2^{-\Delta Ct}$).

Microscopy and Imaging

Invasion assay images were obtained using a Nikon® Eclipse® TE2000-U. Images of two-dimensional cell culture were obtained with a Nikon® Eclipse® TS100. Images of three-dimensional cell culture were obtained using the Nikon® Eclipse® TE2000-E. All images were captured using the NIS Elements Advanced Research software (Nikon Inc. Melville, NY)

Luciferase Assays

SMAD binding element luciferase construct (SBE4-luc) was generated in the lab of Bert Vogelstein (57) and was obtained from Addgene (plasmid 16495). Assays were performed in 96-well plates with 20,000 cells seeded per well. The cells were allowed to attach overnight and were transfected the next day with 200 ng of plasmid DNA per well. Assays were terminated 48 hours after transfection and luminescence was analyzed using the Luciferase Assay System on a Glomax® 20/20 luminometer (Promega, Madison, WI). Luminescence readings were normalized to total protein content in each well.

TGF-β Inhibitors and Ligands

Small molecule inhibitors of the TGF-β signaling pathway were added independently to the cell culture media at various indicated concentrations. A8301 (2 μM), (Stemgent, San Diego, CA) was used according to the manufacturer's recommendations. Recombinant human TGFB1 (#8915) (Cell Signaling Technology) was used 5 ng/mL, unless otherwise indicated. For invasion assays, inhibitors or ligands were added at the same concentration to the serum-free media both in the chamber and in the well. Cells were not pre-treated. For the 3-D cell culture, fresh inhibitors or ligands were added each time the media was changed (every 3-4 days). For standard 2-D cell culture, fresh inhibitors or ligands were added each time the media was changed (every 3-5 days).

Imunocytochemistry

Cells were seeded at 30,000 cells per well in a 24 well plate with a 12mm round poly-lysine coated glass coverslip. Cells after 4% paraformaldehyde fixation, coverslips were washed 3 times in PBS and then blocked with 5% BSA in PBS with 0.3% Triton X-100 for 1 hour at room temperature with gentle shaking. Anti E-cadherin antibody (Cell Signaling, 1:200) was diluted in 1% BSA in PBS with 0.3% Triton X-100 overnight with gentle shaking at 4°C. Coverslips were then washed PBS and incubated for 1 hour at room temperature with anti-rabbit Alexa-Fluor 488 (1:400) in 1%BSA in PBS with 0.3% Triton X-100. Coverslips were washed PBS and mounted using VectaShield™.

Supplementary Material

Refer to Web version on PubMed Central for supplementary material.

Acknowledgements

Grant support: USPHS grants CA140472 and Mayer Mitchell Award (RSS) and CA138850 (LAS).

J. Rostas is a recipient of the American Medical Association Seed Grant 2011.

We thank Dr. Charles V. Clevenger (Northwestern University, Chicago, Illinois) for the gift of the β-casein and LHRE reporters and Dr. Robert Weinberg (Whitehead Institute, Massachusetts) for the gift of HME and HMEC cell lines.

References

1. Price JE. The biology of metastatic breast cancer. Cancer. 1990; 66(6 Suppl):1313–20. Epub 1990/09/15. [PubMed: 2205359]
2. Micalizzi DS, Farabaugh SM, Ford HL. Epithelial-mesenchymal transition in cancer: parallels between normal development and tumor progression. J Mammary Gland Biol Neoplasia. 15(2): 117–34. Epub 2010/05/22. [PubMed: 20490631]
3. Yilmaz M, Christofori G. EMT, the cytoskeleton, and cancer cell invasion. Cancer metastasis reviews. 2009; 28(1-2):15–33. Epub 2009/01/27. [PubMed: 19169796]
4. Greenburg G, Hay ED. Epithelia Suspended in Collagen Gels Can Lose Polarity and Express Characteristics of Migrating Mesenchymal Cells. The Journal of Cell Biology. 1982; 95:333–9. [PubMed: 7142291]
5. Kalluri R. EMT: when epithelial cells decide to become mesenchymal-like cells. J Clin Invest. 2009; 119(6):1417–9. Epub 2009/06/03. [PubMed: 19487817]
6. Thiery JP. Epithelial-mesenchymal transitions in development and pathologies. Curr Opin Cell Biol. 2003; 15(6):740–6. Epub 2003/12/04. [PubMed: 14644200]
7. Lee JM, Dedhar S, Kalluri R, Thompson EW. The epithelial-mesenchymal transition: new insights in signaling, development, and disease. The Journal of cell biology. 2006; 172(7):973–81. Epub 2006/03/29. [PubMed: 16567498]
8. Vincent-Salomon A, Thiery JP. Host microenvironment in breast cancer development: epithelial-mesenchymal transition in breast cancer development. Breast Cancer Res. 2003; 5(2):101–6. Epub 2003/03/13. [PubMed: 12631389]
9. Drasin DJ, Robin TP, Ford HL. Breast cancer epithelial-to-mesenchymal transition: examining the functional consequences of plasticity. Breast Cancer Res. 2011; 13(6):226. Epub 2011/11/15. [PubMed: 22078097]
10. Yates C. Prostate tumor cell plasticity: a consequence of the microenvironment. Adv Exp Med Biol. 2011; 720:81–90. Epub 2011/09/09. [PubMed: 21901620]

11. Yao D, Dai C, Peng S. Mechanism of the mesenchymal-epithelial transition and its relationship with metastatic tumor formation. Mol Cancer Res. 2011; 9(12):1608–20. Epub 2011/08/16. [PubMed: 21840933]
12. Cano CE, Motoo Y, Iovanna JL. Epithelial-to-mesenchymal transition in pancreatic adenocarcinoma. ScientificWorldJournal. 2010; 10:1947–57. Epub 2010/10/05. [PubMed: 20890584]
13. Wang Z, Li Y, Ahmad A, Banerjee S, Azmi AS, Kong D, et al. Pancreatic cancer: understanding and overcoming chemoresistance. Nat Rev Gastroenterol Hepatol. 2011; 8(1):27–33. Epub 2010/11/26. [PubMed: 21102532]
14. Krantz SB, Shields MA, Dangi-Garimella S, Munshi HG, Bentrem DJ. Contribution of epithelial-to-mesenchymal transition and cancer stem cells to pancreatic cancer progression. J Surg Res. 2012; 173(1):105–12. Epub 2011/11/22. [PubMed: 22099597]
15. Kang Y. Pro-metastasis function of TGFbeta mediated by the Smad pathway. J Cell Biochem. 2006; 98(6):1380–90. Epub 2006/04/07. [PubMed: 16598746]
16. Wakefield LM, Piek E, Bottinger EP. TGF-beta signaling in mammary gland development and tumorigenesis. J Mammary Gland Biol Neoplasia. 2001; 6(1):67–82. Epub 2001/07/27. [PubMed: 11467453]
17. Baxley SE, Serra R. Inhibiting breast cancer progression by exploiting TGFbeta signaling. Curr Drug Targets. 2010; 11(9):1089–102. Epub 2010/06/16. [PubMed: 20545612]
18. Taylor MA, Parvani JG, Schiemann WP. The pathophysiology of epithelial-mesenchymal transition induced by transforming growth factor-beta in normal and malignant mammary epithelial cells. J Mammary Gland Biol Neoplasia. 2010; 15(2):169–90. Epub 2010/05/15. [PubMed: 20467795]
19. Bao J, Zervos AS. Isolation and characterization of Nmi, a novel partner of Myc proteins. Oncogene. 1996; 12:2171–6. [PubMed: 8668343]
20. Zhu M, John S, Berg M, Leonard WJ. Functional Association of Nmi with Stat5 and Stat1 in IL-2- and IFNγ-Mediated Signaling. Cell. 1999; 96:121–30. [PubMed: 9989503]
21. Li H, Lee T, Avraham H. A Novel Tricomplex of BRCA1, Nmi, and c-Myc Inhibits c-Myc-induced Human Telomerase Reverse Transcriptase Gene (hTERT) Promoter Activity in Breast Cancer. Journal of Biological Chemistry. 2002; 277(23):20965–73. [PubMed: 11916966]
22. Fillmore RA, Mitra A, Xi Y, Ju J, Scammell J, Shevde LA, et al. Nmi (N-Myc interactor) inhibits Wnt/beta-catenin signaling and retards tumor growth. Int J Cancer. 2009; 125(3):556–64. Epub 2009/04/10. [PubMed: 19358268]
23. Neve RM, Chin K, Fridlyand J, Yeh J, Baehner FL, Fevr T, et al. A collection of breast cancer cell lines for the study of functionally distinct cancer subtypes. Cancer cell. 2006; 10(6):515–27. Epub 2006/12/13. [PubMed: 17157791]
24. Blick T, Widodo E, Hugo H, Waltham M, Lenburg ME, Neve RM, et al. Epithelial mesenchymal transition traits in human breast cancer cell lines. Clinical & experimental metastasis. 2008; 25(6): 629–42. Epub 2008/05/08. [PubMed: 18461285]
25. Debnath J, Muthuswamy SK, Brugge JS. Morphogenesis and oncogenesis of MCF-10A mammary epithelial acini grown in three-dimensional basement membrane cultures. Methods. 2003; 30(3): 256–68. Epub 2003/06/12. [PubMed: 12798140]
26. Zavadil J, Bottinger EP. TGF-beta and epithelial-to-mesenchymal transitions. Oncogene. 2005; 24(37):5764–74. Epub 2005/08/27. [PubMed: 16123809]
27. Postigo AA. Opposing functions of ZEB proteins in the regulation of the TGFbeta/BMP signaling pathway. EMBO J. 2003; 22(10):2443–52. Epub 2003/05/14. [PubMed: 12743038]
28. Joseph MJ, Dangi-Garimella S, Shields MA, Diamond ME, Sun L, Koblinski JE, et al. Slug is a downstream mediator of transforming growth factor-beta1-induced matrix metalloproteinase-9 expression and invasion of oral cancer cells. J Cell Biochem. 2009; 108(3):726–36. Epub 2009/08/15. [PubMed: 19681038]
29. Schmitt E, Hoehn P, Huels C, Goedert S, Palm N, Rude E, et al. T helper type 1 development of naive CD4+ T cells requires the coordinate action of interleukin-12 and interferon-gamma and is inhibited by transforming growth factor-beta. Eur J Immunol. 1994; 24(4):793–8. Epub 1994/04/01. [PubMed: 7908633]

30. Xiao BG, Zhang GX, Ma CG, Link H. Transforming growth factor-beta 1 (TGF-beta1)-mediated inhibition of glial cell proliferation and down-regulation of intercellular adhesion molecule-1 (ICAM-1) are interrupted by interferon-gamma (IFN-gamma). Clin Exp Immunol. 1996; 103(3): 475–81. Epub 1996/03/01. [PubMed: 8608649]
31. Ulloa L, Doody J, Massague J. Inhibition of transforming growth factor-beta/SMAD signalling by the interferon-gamma/STAT pathway. Nature. 1999; 397(6721):710–3. Epub 1999/03/06. [PubMed: 10067896]
32. Xu J, Lamouille S, Derynck R. TGF-beta-induced epithelial to mesenchymal transition. Cell Res. 2009; 19(2):156–72. Epub 2009/01/21. [PubMed: 19153598]
33. Thiery JP, Acloque H, Huang RY, Nieto MA. Epithelial-mesenchymal transitions in development and disease. Cell. 2009; 139(5):871–90. Epub 2009/12/01. [PubMed: 19945376]
34. Nieto MA. The ins and outs of the epithelial to mesenchymal transition in health and disease. Annu Rev Cell Dev Biol. 2011; 27:347–76. Epub 2011/07/12. [PubMed: 21740232]
35. Hugo H, Ackland ML, Blick T, Lawrence MG, Clements JA, Williams ED, et al. Epithelial--mesenchymal and mesenchymal--epithelial transitions in carcinoma progression. J Cell Physiol. 2007; 213(2):374–83. Epub 2007/08/08. [PubMed: 17680632]
36. De Wever O, Pauwels P, De Craene B, Sabbah M, Emami S, Redeuilh G, et al. Molecular and pathological signatures of epithelial-mesenchymal transitions at the cancer invasion front. Histochem Cell Biol. 2008; 130(3):481–94. Epub 2008/07/24. [PubMed: 18648847]
37. De Craene B, Berx G. Regulatory networks defining EMT during cancer initiation and progression. Nature reviews Cancer. 2013; 13(2):97–110. Epub 2013/01/25. [PubMed: 23344542]
38. Creighton CJ, Chang JC, Rosen JM. Epithelial-mesenchymal transition (EMT) in tumor-initiating cells and its clinical implications in breast cancer. J Mammary Gland Biol Neoplasia. 2010; 15(2): 253–60. Epub 2010/04/01. [PubMed: 20354771]
39. Takebe N, Warren RQ, Ivy SP. Breast cancer growth and metastasis: interplay between cancer stem cells, embryonic signaling pathways and epithelial-to-mesenchymal transition. Breast Cancer Res. 2011; 13(3):211. Epub 2011/06/16. [PubMed: 21672282]
40. Fuxe J, Vincent T, Garcia de Herreros A. Transcriptional crosstalk between TGF-beta and stem cell pathways in tumor cell invasion: role of EMT promoting Smad complexes. Cell Cycle. 2010; 9(12):2363–74. Epub 2010/06/04. [PubMed: 20519943]
41. Nawshad A, Lagamba D, Polad A, Hay ED. Transforming growth factor-beta signaling during epithelial-mesenchymal transformation: implications for embryogenesis and tumor metastasis. Cells Tissues Organs. 2005; 179(1-2):11–23. Epub 2005/06/09. [PubMed: 15942189]
42. Tian YC, Fraser D, Attisano L, Phillips AO. TGF-beta1-mediated alterations of renal proximal tubular epithelial cell phenotype. Am J Physiol Renal Physiol. 2003; 285(1):F130–42. Epub 2003/03/20. [PubMed: 12644442]
43. Tian F, Byfield SD, Parks WT, Stuelten CH, Nemani D, Zhang YE, et al. Smad-binding defective mutant of transforming growth factor beta type I receptor enhances tumorigenesis but suppresses metastasis of breast cancer cell lines. Cancer Res. 2004; 64(13):4523–30. Epub 2004/07/03. [PubMed: 15231662]
44. Piek E, Moustakas A, Kurisaki A, Heldin CH, ten Dijke P. TGF-(beta) type I receptor/ALK-5 and Smad proteins mediate epithelial to mesenchymal transdifferentiation in NMuMG breast epithelial cells. J Cell Sci. 1999; 112(Pt 24):4557–68. Epub 1999/11/27. [PubMed: 10574705]
45. Valcourt U, Kowanetz M, Niimi H, Heldin CH, Moustakas A. TGF-beta and the Smad signaling pathway support transcriptomic reprogramming during epithelial-mesenchymal cell transition. Mol Biol Cell. 2005; 16(4):1987–2002. Epub 2005/02/04. [PubMed: 15689496]
46. Miyazono K. Transforming growth factor-beta signaling in epithelial-mesenchymal transition and progression of cancer. Proc Jpn Acad Ser B Phys Biol Sci. 2009; 85(8):314–23. Epub 2009/10/20.
47. Papageorgis P, Lambert AW, Ozturk S, Gao F, Pan H, Manne U, et al. Smad signaling is required to maintain epigenetic silencing during breast cancer progression. Cancer Res. 70(3):968–78. Epub 2010/01/21. [PubMed: 20086175]
48. Saika S, Ikeda K, Yamanaka O, Sato M, Muragaki Y, Ohnishi Y, et al. Transient adenoviral gene transfer of Smad7 prevents injury-induced epithelial-mesenchymal transition of lens epithelium in mice. Lab Invest. 2004; 84(10):1259–70. Epub 2004/07/20. [PubMed: 15258599]

49. Yan X, Liu Z, Chen Y. Regulation of TGF-beta signaling by Smad7. Acta Biochim Biophys Sin (Shanghai). 2009; 41(4):263–72. Epub 2009/04/09. [PubMed: 19352540]
50. Yan X, Chen YG. Smad7: not only a regulator, but also a cross-talk mediator of TGF-beta signalling. Biochem J. 434(1):1–10. Epub 2011/01/29. [PubMed: 21269274]
51. Smith AL, Iwanaga R, Drasin DJ, Micalizzi DS, Vartuli RL, Tan AC, et al. The miR-106b-25 cluster targets Smad7, activates TGF-beta signaling, and induces EMT and tumor initiating cell characteristics downstream of Six1 in human breast cancer. Oncogene. 2012 Epub 2012/01/31.
52. Cocolakis E, Dai M, Drevet L, Ho J, Haines E, Ali S, et al. Smad signaling antagonizes STAT5-mediated gene transcription and mammary epithelial cell differentiation. J Biol Chem. 2008; 283(3):1293–307. Epub 2007/11/21. [PubMed: 18024957]
53. Iwamoto T, Oshima K, Seng T, Feng X, Oo ML, Hamaguchi M, et al. STAT and SMAD signaling in cancer. Histol Histopathol. 2002; 17(3):887–95. Epub 2002/08/10. [PubMed: 12168800]
54. Weng H, Mertens PR, Gressner AM, Dooley S. IFN-gamma abrogates profibrogenic TGF-beta signaling in liver by targeting expression of inhibitory and receptor Smads. J Hepatol. 2007; 46(2): 295–303. Epub 2006/11/28. [PubMed: 17125875]
55. Tsai JH, Donaher JL, Murphy DA, Chau S, Yang J. Spatiotemporal regulation of epithelialmesenchymal transition is essential for squamous cell carcinoma metastasis. Cancer cell. 2012; 22(6):725–36. Epub 2012/12/04. [PubMed: 23201165]
56. Gunasinghe NP, Wells A, Thompson EW, Hugo HJ. Mesenchymal-epithelial transition (MET) as a mechanism for metastatic colonisation in breast cancer. Cancer metastasis reviews. 2012; 31(3-4): 469–78. Epub 2012/06/26. [PubMed: 22729277]
57. Zawel L, Dai JL, Buckhaults P, Zhou S, Kinzler KW, Vogelstein B, et al. Human Smad3 and Smad4 are sequence-specific transcription activators. Mol Cell. 1998; 1(4):611–7. Epub 1998/07/14. [PubMed: 9660945]

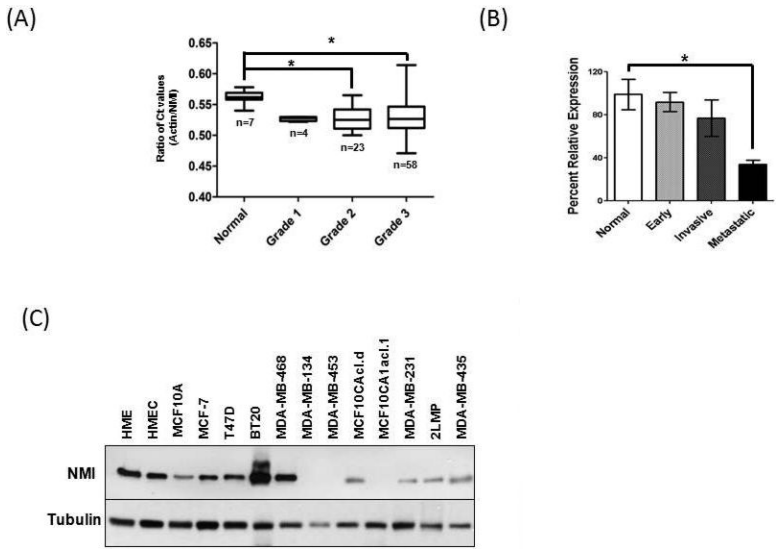

Figure 1. NMI expression decreases in metastatic breast cancer specimens

(A) Human breast cancer patient tissue arrays showing changes in NMI transcript expression between 'normal' tissues and cancer tissues (grades 1-3). C_t values obtained for NMI were normalized to β-actin by calculating a ratio (β-actin C_t/NMI C_t), and these values are plotted on the Y-axis. Significance (* $p<0.05$) was assessed using one-way ANOVA followed by Dunnett's Multiple Comparisons Test.

(B) Percent relative expression is represented from comparison of the immunoreactive scores for NMI staining in breast cancer patient tissue sections from the tissue microarray sides (from CBTR). Staining for normal is designated as 100%. The number of specimens for Normal= 38, Early (Stage 0 and I)= 73, Invasive (Stage II and III)=93 and Metastatic (Stage IV) = 71. Error bars represent ±SEM. Significance (* $p<0.05$) was assessed using one-way ANOVA followed by Dunnett's Multiple Comparisons Test.

(C) NMI expression is reduced in invasive and metastatic cell lines: Breast cell lines were analyzed for level of NMI by western blot analysis.

Table1: Shows the summary of reported epithelial/mesenchymal (E/M) natures of respective cell lines used in Figure 1C, their 3-D growth morphology and Invasive ability. NMI expression levels are depicted as an (*****) using an arbitrary scale of 5* = 100% for NMI expression in HME and HMEC cells. A '-' indicates absence of expression of NMI whereas it indicates absence of information for 3D morphology and invasive ability and E/M nature.

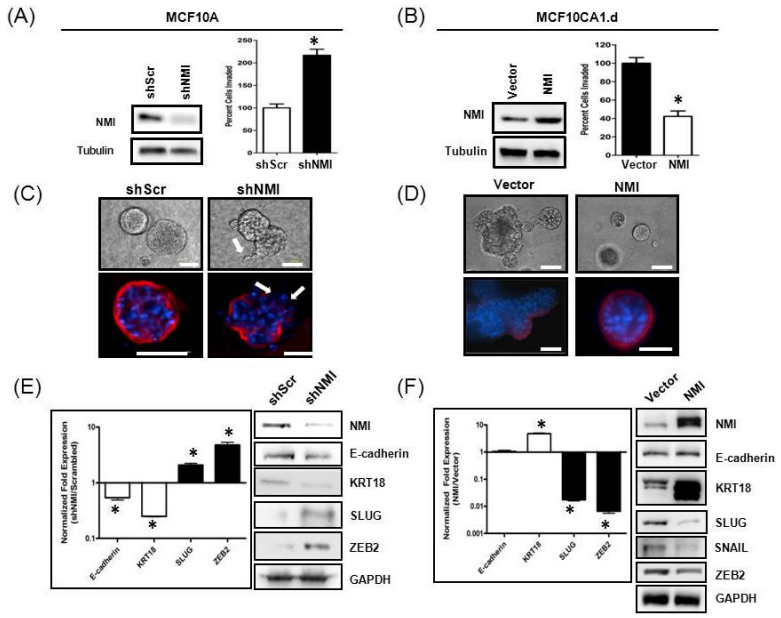

Figure 2. NMI Inhibits Epithelial-Mesenchymal Transitions

(A) MCF10A cells stably transfected with either scrambled control (shScr) or silenced for NMI (sh-NMI) (expression verified by western blot analysis) were analyzed for their ability to invade through Matrigel® invasion chambers (BD Biosciences). P value was calculated using Student's *t*-test.

(B) MCF10CA1.d cells stably transfected with either empty vector control (Vector) or expressing NMI (expression verified by western blot analysis) were analyzed for their ability to invade through Matrigel® invasion chambers (BD Biosciences). P value was calculated using Student's *t*-test.

(C) NMI-silenced (MCF10A-shNMI) or **(D)** NMI expressing (MCF10CA1.d-NMI) cells were grown in three-dimensional matrix comprised of basement membrane extracts (top panels). Cells were grown for 10 days and images captured using phase contrast. Acinar structures were fixed in paraformaldehyde and stained with anti-laminin-V antibody (red) to visualize the basement membrane (bottom panels). Nuclei are stained with DAPI (blue). (Scale bars = 50 μm for MCF10A-shScr and shNMI). For MCF10CAcl.d-Vector Scale bar = 50μm and for MCF10CAcl.d-NMI scale bars = 10 μm. Arrows indicate invasive growth into the matrix and places where basement membrane is compromised.

(E) NMI silencing in MCF10A decreased epithelial markers E-cadherin and keratin 18 and up-regulated expression of mesenchymal transcription factors SLUG and ZEB2. Quantitative RTPCR data is normalized to GAPDH expression and fold changes in expression (log10) are relative to vector control (left panel). Immunoblot analysis of NMI and EMT markers was performed to verify the RT-PCR data. * indicates $p<0.05$

(F) NMI expression in MCF10CA1.d increased expression of epithelial marker keratin 18 and down-regulated expression of mesenchymal transcription factors SLUG, SNAIL and ZEB2. Quantitative RT-PCR data is normalized to GAPDH expression and fold changes in expression (log10) are relative to vector control (left panel). Immunoblot analysis of NMI and EMT markers was performed to verify the RT-PCR data. * indicates $p<0.05$

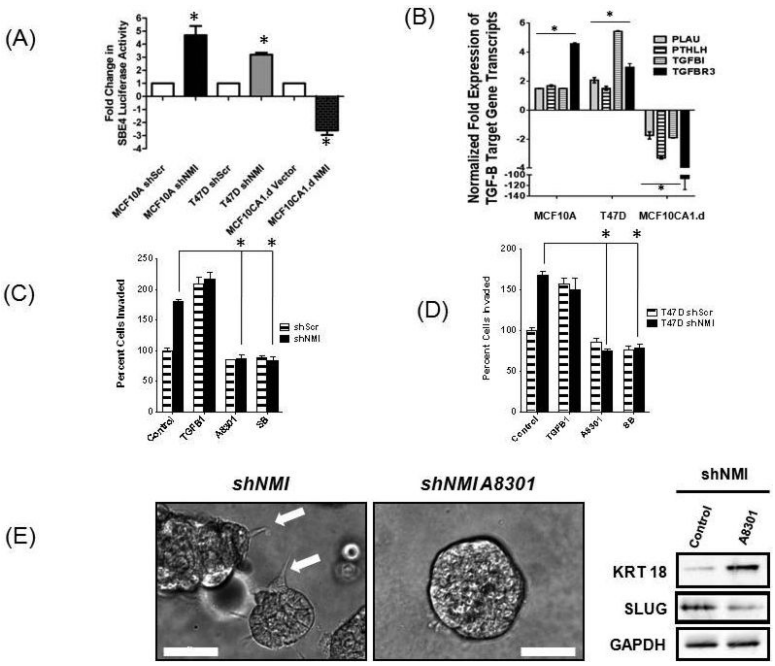

Figure 3. NMI modulates the TGF-β/SMAD signaling pathway

(A) SMAD-mediated transcription inversely correlates with NMI expression as measured by luciferase activity of the SBE4-luc vector in control and shNMI cells (Y axis is linear scale). Stable cell lines were transiently transfected with SBE4-luc and assays were terminated at 48 hours after transfection. Fold expression calculated as NMI/Vector or shNMI/shScr. (***** = $p<0.05$)

(B) Quantitative RT-PCR analysis of TGF-β target genes—PLAU (uPA), PTHLH (PTHRP), TGFBI (BIGH3), TGFBR3 was performed. Normalized fold expression of these genes inversely correlates with NMI expression (Y axis is linear scale). (Note: all values represented by the respective bars are statistically significant from the normalization control. The data is representative of 3 independent experiments with each reading in triplicate.)

(C) Enhancement of *in vitro* invasion through Matrigel induced by NMI silencing in MCF10A and T47D **(D)** is dependent on TGF-β signaling: Invasive ability of TGFB1 treated MCF10A and T47D was compared with shNMI cells. Simultaneously, invasion of shNMI cells treated with A8301 or SB was evaluated. All invasion data is expressed as percent cells invaded with the 'shScr' group arbitrarily set to 100%. Significance (*) was calculated using one-way ANOVA followed by Dunnett's Multiple Comparisons Test. [SB = SB431542]

(E) Enhancement of invasiveness in three-dimensional cell culture of MCF10A-shNMI induced by NMI silencing requires TGF-β signaling. Inhibition of TGF-β signaling (A8301) restricts the formation of invasive structures, as seen in the MCF10A shNMI structures (arrows). Scale bars= 50 μm. Accompanying immunoblot shows reduction in SLUG and increase in Keratin 18 levels upon A8301 treatment.

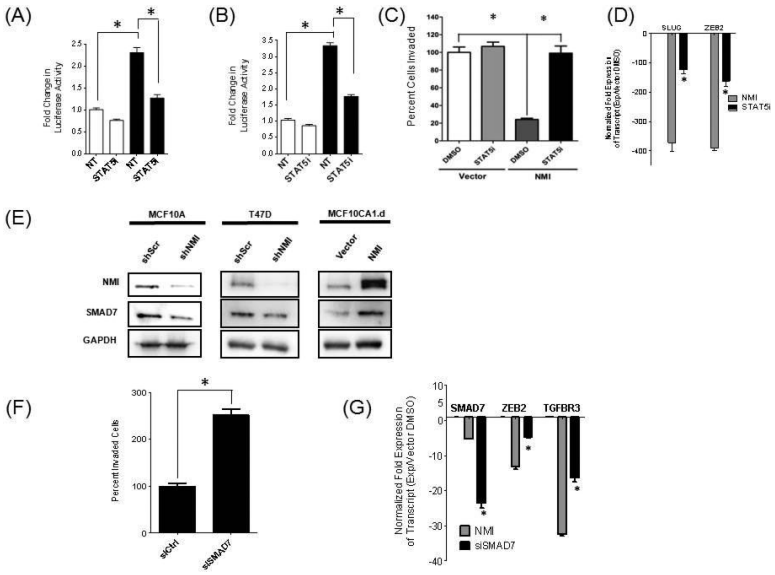

Figure 4. NMI regulates SMAD7 levels

(A) Luciferase activity of LHRE-Luc and β-casein-Luc **(B)** was evaluated 48 hours after transfection in MCF10CA1.d-NMI with and without the treatment of STAT5 inhibitor (STAT5i). Activity is expressed as fold change in comparison with the vector control.

(C) The invasive ability of these same cells with identical treatment was evaluated using modified Boyden chamber assay and is expressed as percent of untreated vector control.

(D) Levels of SLUG and ZEB2 transcript were evaluated in these cells treated with STAT5 inhibitor. The normalized expression is expressed compared to the vector control.

(E) SMAD7 levels from NMI expressor (MCF10CA.1.D) and silenced cells (MCF10A and T47D) were analysed by immunoblot analysis.

(F) Invasive ability of MCF10CA1.d-NMI was evaluated upon silencing SMAD7 expression using siRNA.

(G) The Effect of SMAD7 silencing on ZEB2 and TGFBR3 expression was analyzed by RTQ-PCR. The error bars in all graphs represent SEM. Statistically significant differences are indicated with ***** ($p<0.05$)

Table 1

Shows the summary of reported epithelial/mesenchymal (E/M) natures of respective cell lines used in Figure 1C, their 3-D growth morphology and Invasive ability. NMI expression levels are depicted as an (*) using an arbitrary scale of 5* = 100% for NMI expression in HME and HMEC cells. A '-' indicates absence of expression of NMI whereas it indicates absence of information for 3D morphology and invasive ability and E/M nature.

	Cell line	NMI	Epi(E)/mes(M)	3D Morph	Invasion
1	HME	*****	E	-	-
2	HMEC	*****	E	-	-
3	MCF10A	***	E	sph	Low
4	MCF7	****	E (Vim-/NCad-)	Sph	Low
5	T47D	****	E (Vim-)	Sph	Low
6	BT-20	******	E (Ncad-)		Low
7	MDA-MB-468	****	E/M (Vim-)	sph/grape	Low
8	MDA-MB-134	*	E/M (Vim-)	Grape	Low
9	MDA-MB-453	*	E/M (Vim-/NCad-)	Grape	Low
10	MCF10CA cl. d	**	-	-	-
11	MCF10CA 1a cl.1	*	-	-	-
12	MDA-MB-231	*	M (Vim+/NCad-)	Stellate	High
13	2LMP	*	M (Vim+/NCad-)	Stellate	High
14	MDA-MB-435	*	M (Vim+/NCad+)	Stellate	High